

LIGHT TRANSPORT IN COMPLEX PHOTONIC SYSTEMS

From random lasers to photonic crystals

D.S. WIERSMA, S. GOTTARDO, R. SAPIENZA, S. MUJUMDAR, S. CAVALIERI, M. COLOCCI and R. RIGHINI
*European Laboratory for Non-linear Spectroscopy and INFM
Via Nello Carrara 1, 50019 Sesto-Fiorentino (Florence), Italy
www.complexphotonics.org*

L. DAL NEGRO, C. OTON, M. GHULINYAN, Z. GABURRO
and L. PAVESI
*INFM and Dept. of Physics, Univ. of Trento, via Sommarive
14, Povo (TN), Italy*

F. ALIEV
*Univ. of Puerto Rico, Dept of Physics, PO Box 23343 Rio
Pedros, San Juan, Puerto Rico*

P. JOHNSON, A. LAGENDIJK and W. VOS
*Univ. of Amsterdam, Valckenierstraat 65, 1018 XE Amsterdam,
The Netherlands and Dept. of Appl. Physics & MESA+
Research Inst., Univ. of Twente, P.O. Box 217, Enschede, The
Netherlands*

1. Introduction

The transport of light in complex dielectric materials is a rich and fascinating topic of research. With complex dielectrics we intend dielectric structures with an index of refraction that has variations on a length scales that is very roughly comparable to the wavelength. Such structures strongly scatter light. A possible building block for constructing a complex dielectric is a micro sphere of diameter comparable to the wavelength and of a certain refractive index that is different from its surrounding medium. The single scattering from such a sphere has a rich structure due to internal resonances in the sphere, but its behavior is well-understood and can be calculated using the formalism of Mie-scattering(1). A complex dielectric material can

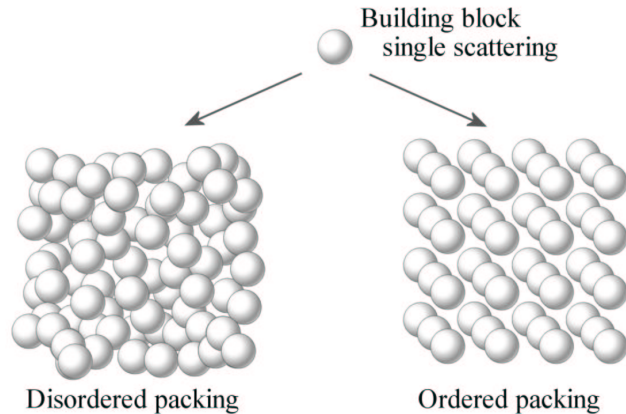
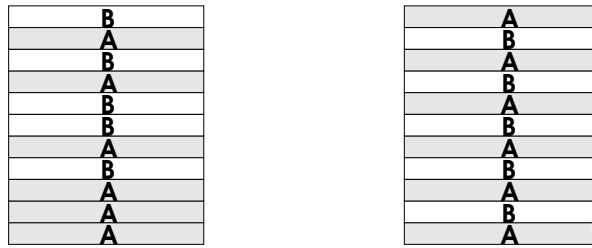


Figure 1. Micro assembly of a complex photonic system. The two extremes are fully disordered assembly (left) leading to random multiple light scattering and ordered assembly (right) resulting in a photonic crystal or possibly a photonic band gap material.

then be realized by micro-assembly of several micro spheres. The spheres can be assembled in various ways with as two opposite possibilities a completely disordered packing and a fully ordered assembly. (See Fig. 1.) Even though the same spheres with the same single scattering properties are used, their cumulative behavior after assembly will depend heavily on the way the spheres are packed together. This is due to the interference between the scattered waves and the way the waves are multiply scattered from one sphere to another. If the spheres are packed according to a crystal-like structure then the interference will be constructive only in certain well defined directions, giving rise to Bragg refraction and reflection. In the disordered case the light waves will perform a random walk from one sphere to the other. The occurrence of interference effects is now less obvious to understand, however also in random systems interference effects turn out to be very important.

Interference of light in random dielectric systems influences the transport of light in a way that is similar to the interference that occurs for electrons when they propagate in disordered conducting materials. As a result, several interference phenomena that are known to occur for electrons appear to have their counterpart in optics as well(2). Interesting examples are correlations and memory effects in laser speckle(3), universal conductance fluctuations of light(4), weak localization(5), and Anderson localization(6). In the case of Anderson localization the interference effects are so strong that the transport comes to a halt and the light becomes localized in randomly distributed modes inside the system. Interference effects in multiple scattering can furthermore be used to study the dynamics



Random stack

Ordered stack

Figure 2. One-dimensional complex photonic systems. By stacking two types of layers (A and B), one can obtain random or ordered one-dimensional structures. In principle any desired stacking rule can be used which allows to explore the regime in between complete order and disorder.

of optically dense colloidal systems(7)

Also in ordered systems interference can give rise to dramatic effects. If the scattering of the spheres that constitute a photonic crystal is strong enough (that is the refractive index contrast between the spheres and their surrounding medium is large and their diameter is resonant with the wavelength) the interference can become destructive in all direction, for a certain range of frequencies. In analogy with the behavior of electrons in semiconductors this range of optical frequencies is referred to as a photonic band gap(8, 9). Inside a photonic band gap the density of light modes becomes zero, which means that even vacuum fluctuations are suppressed. A small impurity inside such a photonic band gap material will give rise to a localized mode around this impurity.

The micro assembly of complex photonic materials as depicted in Fig. 1 is concerned with three dimensional structures. The same principle can be applied to lower dimensional systems. In the case of 1D structures one uses multi-layers of different refractive index and thickness that are stacked either periodically or randomly, or via any other desired packing rule (See Fig. 2). The behavior of light in three dimensional systems is often difficult to describe theoretically. The advantage of lower dimensional structures is that an analytical theoretical description is often available, facilitating the interpretation of experimental results. Results on lower dimensional structures can then be used to learn more about the complex behavior of three dimensional systems.

Whereas the knowledge on the propagation of light waves in completely ordered and disordered structures is now rapidly improving, little is known about the behavior of optical waves in the huge intermediate regime between total order and disorder. An example of a partially ordered system that we will discuss in this paper is a liquid crystal in the nematic phase.

Here the single scattering element is anisotropic due to directional ordering of the liquid crystal molecules along a common axis. Another example that we will discuss is that of light propagation in quasi-crystals in which the scattering elements are assembled in a non-periodic but deterministic way. To construct a quasi-crystal we resort to 1D systems. On the two extremes of order and disorder we will discuss random laser action in amplifying random materials and photonic crystals. In particular we will discuss, in both cases, the role of liquid crystal infiltration to control the scattering strength and thereby the optical properties of these complex systems.

2. Disorder

Light waves in disordered materials perform a random walk which leads to a multiple scattering process. The optical properties of random systems are full of surprises and apart from the before mentioned interference effects several other interesting phenomena occur in these systems that not necessarily depend on interference. Nice examples are optical magneto resistance(10), the photonic Hall effect(11), and optical NTC resistance(12). The knowledge on light diffusion in random systems is furthermore being applied successfully in medical imaging(13).

Of particular interest for photonic applications are disordered materials that provide optical amplification via stimulated emission. If the gain in such amplifying random media becomes larger than the loss through the boundaries, the system exhibits random laser action(14). Such materials can be realized, for instance, by powdering of a laser crystal or by introduction of laser dye in various random media. It was shown that the emission of a random laser is narrow banded(15) and can exhibit laser spiking(16). Theoretical studies furthermore show that a random laser source has interesting photon statistics that are neither those of a regular laser nor those of a common light bulb(17). Recent experiments on Zinc-oxide powders aimed at combining random laser action with Anderson localization effects(18).

A crucial parameter in all multiple light scattering experiments is the scattering strength of the material expressed as the diffusion coefficient or transport mean free path. In many experimental studies one would like to be able to vary the scattering strength of a sample without modifying its other properties. We have found a simple way to obtain external control over the diffusion constant of a random sample. Liquid crystals have the beautiful property that they go through various partially ordered phases when heated. The index of refraction is different in every liquid crystal phase. Of special interest is the nematic phase due to its birefringence in the index of refraction (the index of refraction depends on the propagation direction and polarization of a light wave), which disappears when the liquid crystal

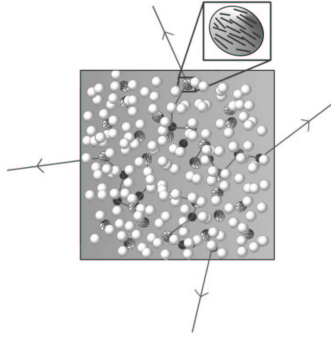


Figure 3. An amplifying disordered material with tunable diffusion coefficient. The laser dye is dissolved in liquid crystal and is excited by an external laser beam to provide optical gain. The refractive index contrast between glass powder and liquid crystal depends on temperature and hence the scattering strength can be temperature controlled.

is heated into the isotropic phase(19). By infiltrating a random sample with a liquid crystal, one can obtain a system of which the diffusion constant strongly depends on temperature(20). This is similar to for instance the concept of smart screens based on polymer dispersed liquid crystals that change their opacity with temperature(21). For a random laser, having control over the diffusion constant has important consequences. The lasing threshold depends on the diffusion constant of the random material. This means that if we have a temperature-dependent diffusion constant, we are able to bring the random laser above and below threshold by changing its temperature.

We realized such a temperature-tunable random laser in the following way. Various types of glasses were ground into a fine powder and sintered under high pressure. The resulting discs of randomly assembled glass grains were infiltrated by a laser dye DCM (Lambdachrome 6500) dissolved in the liquid crystal 4-cyano-4'-n-heptylbiphenyl (7CB) in various concentrations. (See Fig. 3.) The final volume fraction of the liquid crystal in the sample was about 0.26 vol%. The phase sequence of 7CB is crystalline' (15.0) crystalline (30.0) nematic (42.8) isotropic, where the numbers between brackets denote the phase transition temperatures in degrees Celsius.

In Fig. 4 we report the measured diffusion constant and emission spectrum of this tunable random laser material. For experimental details see Ref. (22). From the upper graph in Fig. 4 we see that the diffusion constant diverges (within the experimental accuracy) above the isotropic-nematic phase transition temperature of the liquid crystal. The diffusion constant depends on the refractive index contrast between the liquid crystal and the sintered glass. The refractive indices of SK11 in the 600-800 nm wavelength

range is $n=1.56$ and is hardly temperature dependent. Just above $T = 42.8$ °C, the liquid crystal 7CB is isotropic (I) with a refractive index $n = 1.56$, and this value gradually decreases with rising temperature. Between $T= 30.0$ °C and 42.8 °C, this liquid crystal is nematic (N) and locally birefringent with refractive index $n_o = 1.52$ and $n_e = 1.68$ at $T = 36.0$ °C, and with increasing birefringence at decreasing temperature(23). The observed strong decrease of D when lowering the temperature into the nematic region is therefore due to the enhanced refractive index contrast between liquid crystal and sintered glass. The divergence of the diffusion constant above 42.5 degrees is due to partial refractive index matching between SK11 and 7CB in the isotropic phase. By choosing different liquid crystal / glass combinations, one can obtain different tuning curves for the diffusion constant. Note that the phase behavior of a liquid crystal inside sintered glass is different from the typical phase behavior of bulk liquid crystal and that the nematic-isotropic phase transition is smeared out. This behavior is common for liquid crystals in confined geometries like porous glasses and is due to interaction between the liquid crystal molecules and the surface of the porous host(24).

The random laser emission from the liquid crystal / dye infiltrated sintered glass was characterized by exciting the samples from their front interface with a frequency double Q-switched Nd:YAG laser, operating at 10 Hz repetition rate. The emission spectrum was recorded by collimating the diffuse emission from either the front or the rear sample surface onto the input slit of a single grating spectrometer equipped with a cooled and gated optical multi channel analyzer to provide single shot spectra. At high powers the Q-switch of the laser was operated in single shot mode to prevent cumulative heating (and consequent damage) of the sample. From the lower graph in Fig. 4 we see that indeed there is a strong effect of temperature on emission spectrum. The main feature is a strong decrease of the bandwidth of emission below 42.5 °C. The transition temperature corresponds within the experimental error with the nematic-isotropic phase transition temperature of 7CB. Below this temperature the scattering is strong enough to bring the random laser above threshold. By heating the liquid crystal into the isotropic phase the diffusion constant of the sample increases (the opacity decreases) and the random laser action disappears.

The temperature-tunable random laser provides a new light source of which the emission bandwidth can be temperature controlled. The fact that random laser sources can be made extremely small (tens of microns) and the possibility to work with different spectral tuning curves allows for interesting application as sources in photonic devices, as active displays, and temperature sensitive screens. The tunable random laser can be designed to have its threshold behavior at very specific temperatures, which opens up

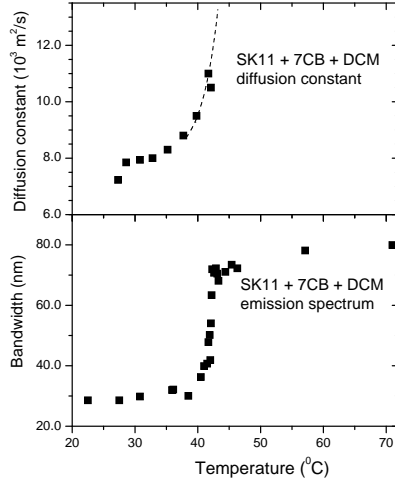


Figure 4. Diffusion constant (upper) and emission spectrum (lower) of sintered SK11 glass powder infiltrated with liquid crystal 7CB and laser dye DCM. Volume fraction liquid crystal in sintered glass 0.26, overall dye concentration in the sample 1.1 mmol/l. Sample thickness 1.3 mm, excitation beam diameter on sample 1.9 mm. Excitation pulse energy 4.5 mJ, pulse duration 14 ns. There is a strong decrease of bandwidth below 42.5 °C. This corresponds to an increase in scattering (lowering of the diffusion constant). Below 42.5 °C the scattering strength of the material becomes large enough to bring the random laser above threshold.

applications in remote temperature sensing especially in the temperature regime of biological processes.

3. Partial ordering

Liquid crystals in the nematic phase are opaque and therefore also give rise to multiple light scattering. This allows coherent backscattering to be observed from large nematic systems(25). The partial ordering of the nematic phase leads to an anisotropic scattering function(26), which makes nematic liquid crystals fundamentally different from common random media. This anisotropy in the scattering cross section leads, for large enough samples, to an anisotropic multiple scattering process, and monodomain nematics are therefore ideal systems to study anisotropic multiple light scattering. Anisotropic light diffusion has recently been observed in cw experiments by Kao *et al.*(27), and later in time-resolved experiments(28), both on large

monodomain nematics. A lot of inspiring theoretical work is available on light propagation in opaque liquid crystals(29).

Comparison between time-resolved transmission measurements and static transmission measurements on monodomain nematic LC's reveals a difference in the observed anisotropy whereas similar measurements on strongly anisotropic disordered GaP networks provide the same value(30). The diffusion constant in an isotropic system can be written as the square of the average step size of the underlying random walk process (after correction for forward scattering) divided by the average time Δt it takes the random walker to cover this step: $D = \ell^2/3\Delta t$. For an anisotropic system like a liquid crystal the step length and time, in principle, both become anisotropic and their value will depend on the propagation direction of the random walker. However, for sufficiently large systems, one should assume that Δt takes some average value, which allows to write the perpendicular and parallel values of the diffusion constant in terms of one average Δt . (This is actually a necessary requirement to make the diffusion approximation in the first place.) It is clear that under these assumptions the *anisotropy* in the diffusion constant D_{\perp}/D_{\parallel} can be calculated from the *anisotropy* in the transport mean free path, since then we can write: $D_{\parallel}/D_{\perp} = \ell_{\parallel}^2/\ell_{\perp}^2$. In static experiments one measures the transport mean free path of the system whereas the diffusion constant is a dynamical property and can be measured only in time-resolved experiments. However, under the assumptions above, one can derive the *anisotropy* in the diffusion constant from the measured *anisotropy* in the mean free path, as was done in the static experiments of Refs. (27, 28, 30). The above assumptions might not be valid for multiple scattering processes with non-Gaussian statistics (like Levy-flights) in which the diffusion approximation breaks down or for systems with long range correlations. It is not clear if the diffusion approximation is correct at all for nematic liquid crystals. An unambiguous way to measure the transport mean free path is via coherent backscattering(5) which is, however, technically very challenging for liquid crystals due to their long mean free paths. The angular resolution in the measurements reported in Ref. (25) was not sufficient to resolve the width of the backscattering cone and therefore did not allow to determine the mean free paths.

4. Quasi-crystals

Quasi-crystals form another class of fascinating systems in between fully ordered and completely disordered. Quasi-crystals are non-periodic structures that are constructed following a deterministic generation rule(31). If made from dielectric material, the resulting structure has fascinating optical properties. Quasi-crystals of the Fibonacci type, for instance, exhibit

an energy spectrum that consists of a self-similar Cantor set with zero Lebesgue measure(32). The transmission spectrum of a Fibonacci system also contains forbidden frequency regions called ‘pseudo band gaps’ similar to the band gaps of a photonic crystal(33). In the frequency regime outside these Fibonacci band gaps, the light waves are critically localized. In contrast with the fully disordered (Anderson) localized case, these critically localized states decay weaker than exponentially, most likely by a power law, and have a rich self-similar structure(34). This makes these systems very interesting for light localization studies, as proposed by Kohmoto et al.(35). The first Fibonacci sequence for electron transport studies was realized by Merlin et al.(36), which was followed by several experiments and theoretical studies on electron propagation in these systems(37). The experimental work on light transport in this fascinating class of structures is limited so far. Important pioneering experiments were performed by Gellerman et al.(38) who observed self-similarity in the transmission spectrum of Fibonacci dielectric multi-layers and by Hattori et al.(39) who measured the Fibonacci dispersion curves.

A Fibonacci quasi-crystal is a deterministic aperiodic structure that is formed by stacking two different compounds A and B according to the Fibonacci generation scheme: $S_{j+1} = \{S_{j-1}S_j\}$ for $j \geq 1$; with $S_0 = \{B\}$ and $S_1 = \{A\}$. The lower order sequences are $S_2 = \{BA\}$, $S_3 = \{ABA\}$, $S_4 = \{BAABA\}$, etc. We have realized one-dimensional Fibonacci structures from porous Silicon by stacking 233 layers using two types of layers A and B according to the Fibonacci packing scheme, leading to a 12-th order Fibonacci system(40). To study the transport properties of the Fibonacci band edge modes we have performed time-resolved transmission experiments using a fixed Mach-Zehnder interferometer coupled with a Michelson interferometer to measure the interferometric cross correlation of the transmitted pulse with a reference pulse. This technique provides both the amplitude and phase information of the transmission through the sample. For further details we refer to Ref. (41). As laser source we used a tunable parametric oscillator, pumped by a fast (200 fs pulse duration) Ti:Sapphire laser.

The measured pulse envelope of the time-resolved transmittance is plotted in Fig. 5. The transmission spectrum of the sample is given in the top graph, together with the laser spectra corresponding to three time-resolved measurements. When the incoming pulse is resonant with one transmission peak, the pulse is significantly delayed and stretched (I). This stretching becomes surprisingly strong close to the band edge (III). In addition to the delay and stretching, when the spectrum of the laser pulse overlaps with two adjacent narrow transmission modes a strongly oscillatory behavior is observed (II). These oscillations can be interpreted as due to beating

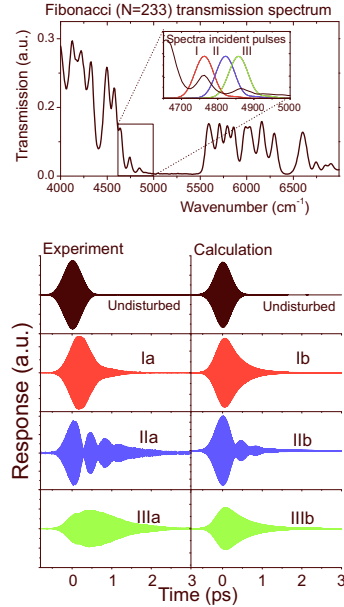


Figure 5. Experimental data and calculation of the transmission through Fibonacci samples at four different frequencies. Also the undisturbed pulse which has only passed through the Si substrate and not the Fibonacci sample is plotted for comparison. When the laser pulse is resonant with one band edge state the transmitted intensity is strongly delayed and stretched. When two band edge states are excited, mode beating is observed. The top graph shows the transmission spectrum of the sample together with the three laser spectra corresponding to the measurements I-III

between individual band edge modes. Indeed the frequency of the oscillations corresponds to the frequency difference between the peaks in the transmission spectrum. The strong pulse delay leads to a group velocity suppression that turns out to be three times larger than that observed in three dimensional photonic crystals made of colloidal polystyrene spheres(42). The response in the time domain can be calculated from the inverse Fourier transformation of the product of the complex transmission coefficient and the incident pulse envelope(43). Taking exactly the experimental incidence pulse envelope (FWHM: 63 cm^{-1}), coherent beating and pulse stretching are very well reproduced, as can be seen from the theoretical curves in the right column of Fig. 5.

The large group velocity reduction and pulse stretching that we find experimentally is only observed close to the band edge. The band edge is also the region where the periodic like features (band gap) of the Fibonacci system go over into its disorder properties (critically localized states). In Fig. 6 we have plotted the calculated intensity distribution inside the sample as a function of frequency. The Fibonacci pseudo band gap is clearly visible

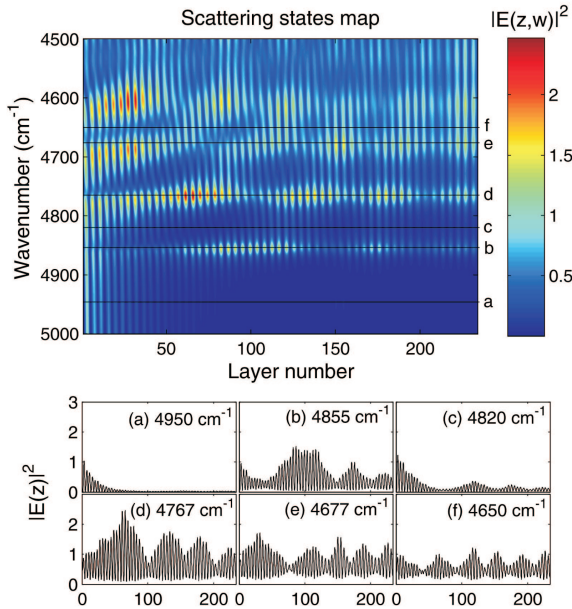


Figure 6. Calculated intensity distribution inside the Fibonacci quasi-crystal sample as used in the experiments. X-axis: layer number, y-axis: wavenumber of the incident light. This means that any horizontal cut through the graph represents an intensity distribution at one specific frequency. The insets show the intensity distributions at several frequencies. (Horizontal cuts are indicated by black lines.) The input intensity of the electric field has been normalized to unity. Note that the intensity inside the sample can become larger than one, due to internal resonances.

in the lower part of the plot. Just above the pseudo band gap the band edge modes are visible. The insets show the normalized field intensity distributions for several frequencies. The incoming field is normalized to 1. The first inset (a) shows the exponentially decaying intensity of light that is incident in the band gap region, whereas the other insets (b-f) show the intensity distribution in the band edge region when moving away from the band gap. (Insets (b) and (d) correspond to the first two transmission maxima whereas (c) is taken in between these maxima.) The first and second order band edge resonances (with only one respectively two maxima) are suppressed due to the minor drift in layer thickness and porosity.

The resonances of the band edge states are sharp enough to allow for mode beating when adjacent modes are excited simultaneously, as observed in the experiments. The distributions that we find in Fig. 6 have a notable similarity to the band edge resonances occurring in photonic crystals(44) but are less regular. Band edge resonances in (finite-size) photonic crystals are due to a transient standing wave that is formed inside the sample and can temporarily store a substantial amount of energy. This is consistent

with a large group velocity reduction and strong pulse stretching as observed in our experiments. Since this transient standing wave is formed from reflection by the sample boundaries, it has the characteristic intensity distribution of the various harmonics of a standing wave. Band edge resonances in photonic crystals are not localized states since their extension scales linearly with the system size and they do not decay to zero(44). In contrast, the Fibonacci band edge resonances will decay via a power law due to their critically localized nature. Fibonacci systems can provide an interesting alternative to regular photonic crystals for the realization of photonic devices like e.g. optical filters with a self-similar spectrum and a high wavelength selectivity in the band edge region. Another interesting future application of these materials could be realized in the field of random lasers, where the Fibonacci band edge resonances could serve as a new type of complex cavity that provides the feedback for laser action.

5. Photonic crystals with liquid crystal infiltration

If we assemble a complex dielectric material in a periodic way we obtain a crystal like structure that under appropriate conditions can exhibit a photonic band gap. For applications of photonic band gap materials as photonic devices it is very useful to have external control over their band structure. In section 2 we have seen how liquid crystal infiltration can be used to tune the diffusion constant of a disordered complex system. If liquid crystal infiltration is used in (ordered) photonic crystal structures it could allow to control its photonic band gap, as was proposed by Busch and John(45). Temperature control of the band gap of two dimensional photonic crystals has been demonstrated experimentally, and shifts as large as 70 nm in the central wavelength of the band gap were observed(46). Electric field tuning of the photonic stop band in opals was explored experimentally but the effects observed so far were limited by surface anchoring of the liquid crystal(47, 48).

One might expect that inverse opal structures, having spherical voids, are favorable for external field switching since a spherical void does not impose a preferred alignment direction. In addition, at fixed lattice constant, the inverse opal voids are bigger than those of a direct opal. To further exploit the possibilities of electric field tuning of photonic crystals we characterized the stop band of infiltrated titania inverse opals.

The titania inverse opals were based on self-organized direct opals of monodispers polystyrene spheres. These direct opals were infiltrated with TiO_2 , via a precursor solution (tetra-propoxy-titane). Calcination of the TiO_2 by heating to 450 °C subsequently also removes the polystyrene and leaves a clean titania inverse opal (air spheres in a TiO_2 backbone). See

for more details Ref. (49). The lattice constant a of the resulting titania inverse opals was 451 nm and their pore radius was 160 nm.

The titania inverse opal was infiltrated overnight with the liquid crystals 5CB or E7. The infiltrated samples were mounted between two glass slides coated with a thin transparent layer of Indium doped Tin Oxide (ITO) on the glass surface facing the sample. Before mounting the glass slides, part of the ITO coating was carefully removed in order to avoid regions of facing ITO layers without sample in between. The sample thickness equals the distance between glass plates and ranges from 0.2 to 0.5 mm in our case.

The electric conductance of the tin oxide allows to apply an electric field over the sample perpendicular to the sample plane. Without the electric field the optical properties of the sample are expected to be isotropic, whereas at high enough field the nematic director should obtain some global alignment and hence the stop band of the infiltrated photonic crystal is expected to shift towards higher wavelengths. Since the sample is a very good insulator (much better than air), and facing ITO layers always have sample material in between, we can apply an electric field as high as 24 kV/ μm to the sample (ac at 500 Hz).

A good way to characterize the stop band of a photonic crystal is via angular and wavelength resolved reflection measurements. A stop band appears as a wavelength regime where the reflectivity is high. In Fig. 7 we report angular resolved reflection spectra of a liquid crystal infiltrated titania inverse opal. If the system were to exhibit a complete photonic band gap, there would exist a wavelength region in which all reflection spectra overlap. This is not the case for our liquid crystal infiltrated samples as can be seen in Fig. 7. Although the density of states in un-infiltrated titania inverse opals is strongly reduced(50), after liquid crystal infiltration the refractive index contrast is diminished. This is the reason that the stop bands in Fig. 7 are not overlapping.

When we apply the electric field, the position of the stop bands is not changed considerably within the accuracy of our experiment (resolution about 1 nm). When we apply the maximum electric field of 24 V/ μm we observe only a minor increase of the reflected intensity. (See inset of Fig. 7.) These data might indicate also a tiny red shift of the reflection peak which however can not be considered significant. This increase and red shift could be mistakenly interpreted as a switching effect of the stop band of the sample by the electric field. We observe that it sets in slowly after applying the electrical field, which suggests an interpretation in terms of a heating effect of the sample and not a field effect. Heating effects on the reflection spectra from infiltrated photonic crystals were studied by e.g. Mertens et al.(51). Apparently the alignment of the liquid crystal due to the electric field is too small to induce any appreciable global anisotropy in our system.

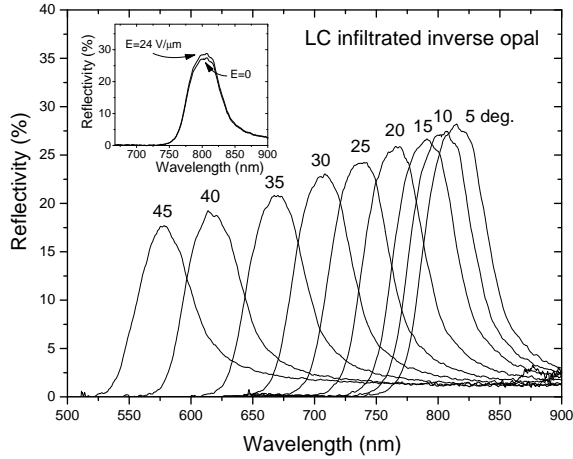


Figure 7. Reflection spectra of titania inverse opals infiltrated with the liquid crystal E7. The emission of a broad-band lamp was collimated via an optical fiber on the sample (spot size on the sample surface $100 \mu\text{m}$), and the reflected light was detected via an optical fiber by a spectrometer (spectral resolution 1 nm). The incoming and detection angle are equal and given in the graph with respect to the sample normal. The inset shows the tiny increase of the reflection peak at 10 degrees upon switching on the electric field. (Field strength $24 \text{ V}/\mu\text{m}$.)

A possible improvement of the coupling with the external electric (or even magnetic) field could be obtained by a low-concentration addition of highly dielectric (or magnetic) nano rods suspended in the liquid crystal.

6. Conclusions

We have discussed several examples of light transport in complex photonic structures, going from disordered systems to partially ordered materials, quasi-crystals, and fully ordered systems. The vast regime between completely ordered and disordered structures is very rich and has yet to be fully explored. Liquid crystals have been a common theme in several sections of this paper, either as a system to study multiple light scattering or as a way to obtain control over the optical properties of porous photonic materials via infiltration. The transport of light in these various complex structures is very interesting from a fundamental point of view and these new materials could find fascinating applications as photonic devices, in telecommunications, and possibly even in future optical computing.

7. Acknowledgements

We wish to thank Zhao-Qing Zhang and Prof. V. Freilikher. for inspiring discussions, Anna Vinattieri and Daniele Alderighi for help with the time-resolved experiments, and Lydia Bechger for her work on the realization of titania inverse opals. This work was financially supported by the European community (contract number HPRI-CT1999-00111) and by the Istituto Nazionale di Fisica della Materia (PAIS project RANDS and PRA project PHOTONIC).

References

1. See e.g. H.C. van de Hulst, *Light scattering by small particles* (Dover, New York, 1981).
2. See for instance: P. Sheng, *Introduction to Wave Scattering, Localization, and Mesoscopic Phenomena* (Academic Press, San Diego, 1995).
3. I. Freund, M. Rosenbluh, and Shechao Feng, Phys. Rev. Lett. **61**, 2328 (1988); Shechao Feng, Ch. Kane, P.A. Lee, and A. D. Stone, Phys. Rev. Lett. **61**, 834 (1988); N. Garcia and A.Z. Genack, Phys. Rev. Lett. **63**, 1678 (1989); M.P. van Albada, J.F. de Boer, and A. Lagendijk, Phys. Rev. Lett. **64**, 2787 (1990). P. Sebbah, B. Hu, A.Z. Genack, R. Pnini, and B. Shapiro, Phys. Rev. Lett. **88**, 123901 (2002).
4. F. Scheffold and G. Maret, Phys. Rev. Lett. **81**, 5800 (1998).
5. Y. Kuga and A. Ishimaru, J. Opt. Soc. Am. A **8**, 831 (1984); M.P. van Albada and A. Lagendijk, Phys. Rev. Lett. **55**, 2692 (1985); P.E. Wolf and G. Maret, Phys. Rev. Lett. **55**, 2696 (1985).
6. S. John, Phys. Rev. Lett. **53**, 2169 (1984); P.W. Anderson, Philos. Mag. B **52**, 505 (1985); R. Dalichaouch, J.P. Armstrong, S. Schultz, P.M. Platzman, and S.L. McCall, Nature **354**, 53 (1991); A.Z. Genack and N. Garcia, Phys. Rev. Lett. **66**, 2064 (1991); D.S. Wiersma, P. Bartolini, A. Lagendijk, and R. Righini, Nature **390**, 671 (1997); A.A. Chabanov and A.Z. Genack, Phys. Rev. Lett. **87**, 233903 (2001).
7. G. Maret and P.E. Wolf, Z. Phys. B **65**, 409 (1987); D.J. Pine, D.A. Weitz, P.M. Chaikin, and E. Herbolzheimer, Phys. Rev. Lett. **60**, 1134 (1988); S. Fraden and G. Maret, Phys. Rev. Lett. **65**, 512 (1990).
8. E. Yablonovitch, Phys. Rev. Lett. **58**, 2059 (1987); S. John, Phys. Rev. Lett. **58**, 2486 (1987).
9. *Photonic Bandgap Materials*, edited by C.M. Soukoulis (Kluwer, Dordrecht, 1996); J.D. Joannopoulos, R.D. Meade, and J.N. Winn, *Photonic Crystals* (Princeton University Press, Princeton, NJ, 1995).
10. A. Sparenberg, G.L.J.A. Rikken, and B.A. van Tiggelen, Phys. Rev. Lett. **79**, 757 (1997).
11. B.A. van Tiggelen, Phys. Rev. Lett. **75**, 422 (1995); G.L.J.A. Rikken and B.A. van Tiggelen, Nature **381**, 54 (1996).
12. D.S. Wiersma, Mol. Cryst. and Liq. Cryst. **375**, 15 (2002).
13. A. Yodh and B. Chance, Physics Today **48-3**, 34 (1995).
14. V.S. Letokhov, Zh. Eksp. Teor. Fiz. **53**, 1442 (1967) [Sov. Phys. JETP **26**, 835 (1968)]; A.Y. Zyuzin, Phys. Rev. E **51**, 5274 (1995); S. John and G. Pang, Phys. Rev. A **54**, 3642 (1996); D.S. Wiersma and A. Lagendijk, Phys. Rev. E **54**, 4256 (1996); G.A. Berger, M. Kempe, and A.Z. Genack, Phys. Rev. E **56**, 6118 (1997);

- Xunya Jiang and C.M. Soukoulis, *Phys. Rev. Lett.* **85**, 70 (2000). G. van Soest, F.J. Poelwijk, R. Sprik, and A. Lagendijk, *Phys. Rev. Lett.* **86**, 1522 (2001).
15. N.M. Lawandy, R.M. Balachandran, A.S.L. Gomes, and E. Sauvin, *Nature* **368**, 436 (1994); but see also the discussion on weak scattering in: D.S. Wiersma, M. van Albada, A. Lagendijk, *Nature* **373**, 203 (1995).
 16. C. Gouedard, D. Husson, C. Sauteret, F. Auzel, and A.J. Migus, *J. Opt. Soc. Am. B* **10**, 2358 (1993).
 17. C.W.J. Beenakker, *Phys. Rev. Lett.* **81**, 1829 (1998).
 18. H. Cao, Y.G. Zhao, S.T. Ho, E.W. Seelig, Q.H. Wang, and R.P.H. Chang, *Phys. Rev. Lett.* **82**, 2278 (1999); H. Cao, Y. Ling, J.Y. Xu, C.Q. Cao, and Prem Kumar, *Phys. Rev. Lett.* **86**, 4524 (2001); but see also Y. Sun, J.B. Ketterson, and G.K.L. Wong, *Appl. Phys. Lett.* **77**, 2322 (2000).
 19. P.G. de Gennes and J. Prost, *The Physics of Liquid Crystals* 2nd edition (Oxford, New York, 1993); S. Chandrasekhar, *Liquid Crystals* (Cambridge Univ. Press, Cambridge, 1977).
 20. D.S. Wiersma, M. Colocci, R. Righini, and F. Aliev, *Phys. Rev. B* **64**, 144208 (2001).
 21. See for instance *Liquid Crystal Dispersions*, P. S. Drzaic, (World Scientific, Singapore, 1995); A. Mertelj, L. Spindler, and M. Copic, *Phys. Rev. E* **56**, 549 (1997); J.H.M. Neijzen, H.M.J. Boots, F.A.M.A. Paulissen, M.B. van der Mark, and H.J. Cornelissen, *Liq. Cryst.* **22**, 255 (1997); L. Leclercq, U. Maschke, B. Ewen, X. Coqueret, L. Mechernene, and M. Benmouna, *Liq. Cryst.* **26**, 415 (1999); T. Bellini, N.A. Clark, V. Degiorgio, F. Mantegazza, and G. Natale, *Phys. Rev. E* **57**, 2996 (1998).
 22. D.S. Wiersma and S. Cavalieri, *Nature* **414**, 708 (2001); D.S. Wiersma and S. Cavalieri, *Phys. Rev. E* **66**, 056612 (2002).
 23. Refractive index values at $\lambda = 632.8$ nm. See D.A. Dunmur, M.R. Manterfield, W.H. Miller, and J.K. Dunleavy, *Mol. Cryst. Liq. Cryst.* **45**, 127 (1978).
 24. *Liquid Crystals in Complex Geometries Formed by Polymer and Porous Networks*, edited by G.P. Crawford and S. Zumer (Taylor & Francis, London, 1996); T. Bellini, N.A. Clark, C.D. Muzny, L. Wu, C.W. Garland, D.W. Schaefer, and B.J. Olivier, *Phys. Rev. Lett.* **69**, 788 (1992).
 25. D.V. Vlasov, L.A. Zubkov, N.V. Orekhova, and V.P. Romanov, *Pis'ma Zh. Eksp. Teor. Fiz.* **48**, 86 (1988) [*JETP Lett.* **48**, 91 (1988)]; H.K.M. Vithana, L. Asfaw, and D.L. Johnson, *Phys. Rev. Lett.* **70**, 3561 (1993).
 26. D. Langevin, *Solid State Comm.* **14**, 435 (1974); D. Langevin and M.-A. Bouchiat, *J. Phys. (Paris) C* **1**, 197 (1975); A.Y. Val'kov and V.P. Romanov, *Zh. Eksp. Teor. Viz.* **82**, 1777 (1982) [*Sov. Phys. JETP* **56**, 1028 (1983)].
 27. M.H. Kao, K.A. Jester, A.G. Yodh, and P.J. Collings, *Phys. Rev. Lett.* **77**, 2233 (1996).
 28. D.S. Wiersma, A. Muzzi, M. Colocci, and R. Righini, *Phys. Rev. Lett.* **83**, 4321 (1999).
 29. V.P. Romanov and A.N. Shalaginov, *Opt. Spectrosc. (USSR)* **64**, 774 (1988); B.A. van Tiggelen, R. Maynard, and A. Heiderich, *Phys. Rev. Lett.* **77**, 639 (1996); H. Stark and T.C. Lubensky, *Phys. Rev. Lett.* **77**, 2229 (1996); B.A. van Tiggelen and H. Stark, *Rev. Mod. Phys.* **72**, 1017 (2000).
 30. P.M. Johnson, B.P.J. Bret, J.G. Rivas, J.J. Kelly, and A. Lagendijk, *Phys. Rev. Lett.* **89**, 243901 (2002).
 31. T. Fujiwara and T. Ogawa, *Quasicrystals* (Springer Verlag, Berlin, 1990).
 32. Godfrey Gumbs and M.K. Ali, *Phys. Rev. Lett.* **60**, 1081 (1988);

33. See e.g. Franco Nori and J. P. Rodriguez, *Phys. Rev. B* **34**, 2207 (1986); R.B. Capaz, B. Koiller, and S.L.A. de Queiroz, *Phys. Rev. B* **42**, 6402 (1990).
34. T. Fujiwara, M. Kohmoto, and T. Tokihiro, *Phys. Rev. B* **40**, 7413 (1989); C.M. Soukoulis and E.N. Economou, *Phys. Rev. Lett.* **48**, 1043 (1982).
35. Mahito Kohmoto, Bill Sutherland, and K. Iguchi, *Phys. Rev. Lett.* **58**, 2436 (1987); B. Sutherland and M. Kohmoto, *Phys. Rev. B* **36**, 5877 (1987).
36. R.Merlin, K. Bajema, R. Clarke, F.Y. Juang, and P.K. Bhattacharya, *Phys. Rev. Lett.* **55**, 1768 (1985).
37. J.B. Sokoloff *Phys. Rev. Lett.* **58**, 2267 (1987); Ch.Wang and R.A. Barrio, *Phys. Rev. Lett.* **61**, 191 (1988); E. Maciá and F. Domínguez-Adame, *Phys. Rev. Lett.* **76**, 2957 (1996); F. Piéchon, *Phys. Rev. Lett.* **76**, 4372 (1996); X. Huang and Ch. Gong, *Phys. Rev. B* **58**, 739 (1998); F. Steinbach, A. Ossipov, Tsampikos Kottos, and T. Geisel, *Phys. Rev. Lett.* **85**, 4426 (2000).
38. W. Gellermann, M. Kohmoto, B. Sutherland, and P.C. Taylor, *Phys.Rev.Lett.***72**, 633 (1994).
39. T. Hattori, N. Tsurumachi, S. Kawato, and H. Nakatsuka, *Phys. Rev. B* **50**, 4220, (1994).
40. L. dal Negro, C.J. Oton, Z. Gaburro, L. Pavesi, P. Johnson, A. Lagendijk, R. Righini, M. Colocci, D.S. Wiersma, *Phys. Rev. Lett.* **90**, xxxx (2003).
41. R.H.J. Kop and R. Sprik, *Rev. Sci. Instrum.* **66**, 5459 (1995).
42. A. Imhof, W.L. Vos, R. Sprik, and A. Lagendijk, *Phys. Rev. Lett.* **83**, 2942 (1999).
43. F.L. Pedrotti and L.S. Pedrotti, *Introduction to Optics* (Prentice-Hall, 1987); A. Kavokin, G. Malpuech, A. Di Carlo, P. Lugli, and F. Rossi, *Phys. Rev. B* **61**, 4413 (2000).
44. M. Scalora et al., *Phys. Rev. E* **54**, R1078 (1996).
45. K. Busch and S. John, *Phys. Rev. Lett.* **83**, 967 (1999).
46. K. Yoshino, Y. Shimoda, Y. Kawagishi, K. Nakayama, and M. Ozaki, *Appl. Phys. Lett.* **75**, 932 (1999); S.W. Leonard, J.P. Mondia, H.M. van Driel, O. Toader, S. John, K. Busch, A. Birner, U. Gosele, and V. Lehmann, *Phys. Rev. B* **61**, R2389 (2000).
47. D. Kang, J.E. Maclennan, N.A. Clark, A.A. Zakhidov, and R.H. Baughman, *Phys. Rev. Lett.* **86**, 4052 (2001).
48. Y. Shimoda, M. Ozaki, and K. Yoshino, *Appl. Phys. Lett.* **79**, 3627 (2001); Q.B. Meng, C.H. Fu, S. Hayami, Z.Z. Gu, O. Sato, and A. Fujishima, *J. Appl. Phys.* **89**, 5794 (2001); P. Mach, P. Wiltzius, M. Megens, D.A. Weitz, Keng-hui Lin, T.C. Lubensky, and A.G. Yodh, *Phys. Rev. E* **65**, 031720 (2002).
49. J.E.G.J. Wijnhoven and W.L. Vos, *Science* **281**, 802 (1998); J.E.G.J. Wijnhoven, L. Bechger, and W.L. Vos, *Chem. Mater.* **13**, 4486 (2001).
50. A.F. Koenderink, L. Bechger, H.P. Schriemer, A. Lagendijk, and W.L. Vos, *Phys. Rev. Lett.* **88**, 143903 (2002).
51. G. Mertens, T. Röder, R. Schweins, K. Huber, and Heinz-S. Kitzerow, *Appl. Phys. Lett.* **80**, 1885 (2002).